A Second Order Initial Value Solution of Two-dimensional Sloshing in Rectangular Tanks

Olav F. Rognebakke and Odd M. Faltinsen
Department of Marine Hydrodynamics
Norwegian University of Science and Technology
N-7034 Trondheim, Norway

Environmental concern has led to requirements about double bottoms and skin in new tankers. It is desirable to save steel, and this has led to wide oil tanks that can be smooth inside. The most violent fluid motions inside the tank occur in the vicinity of the highest natural period of the fluid motion. When the tank is smooth, viscous effects are not important and potential flow theory can be used. Nonlinear free surface effects are significant.

Experiments have been carried out with forced harmonic sway oscillations of a rectangular smooth tank. The oscillation frequencies are close to the lowest natural frequency of the fluid motion inside the tank. The results show a clear beating effect that does not die out. A frequency analysis shows the presence of both the lowest natural frequency and the forced oscillation frequency. This implies that a steady-state solution as presented by Faltinsen [1] and Solaas and Faltinsen [2] cannot be used. Nonlinear effects are clearly present in the experimental results. A theoretical solution is derived to explain the experimental findings. The response is assumed to be $\mathcal{O}(\epsilon)$, where the small parameter ϵ characterizes the order of magnitude of the forced sway amplitude relative to the breadth of the tank. A second-order solution in terms of ϵ is derived. This is not valid at resonance. It then seems necessary to assume that the response is of lower order than the excitation. The steady-state solution in [1] and [2] assumes the response to be $\mathcal{O}(\epsilon^{1/3})$. The fluid is assumed incompressible and the flow two-dimensional and irrotational so that there exists a velocity potential Φ_T satisfying the 2-D Laplace equation in the fluid domain. The rectangular tank is oscillating harmonically in sway. The coordinate system is shown in Fig. 1. The tank position relative to equilibrium is $\eta = \epsilon_0 \sin(\omega t)$. The first order potential Φ_1 satisfies the linearized free surface condition and the body boundary conditions on the side walls and the tank bottom. The transient is kept due to a very small damping. The level of damping can be estimated by the use of formulas given in Keulegan [3]. For the tank dimensions used in the experiments it will be less than 0.3% of the critical damping for a linear standing wave at the highest natural period. This means the amplitude is halved after $\approx$ 100 oscillation cycles. Since potential theory is used, the damping is zero. The initial conditions $\Phi_1 = 0$ and $\partial\Phi_1/\partial t = 0$ on the mean free surface are used. The first order potential is written as $\Phi_1 = \phi_1 + \phi_c$ where $\phi_c = Ax\cos(\omega t)$ is associated with the forced oscillation. The expression for ϕ_1 is

$$\phi_1 = \sum_{n=0}^{\infty} [A_n \cos(\omega_n t) + C_n \cos(\omega t)] \sin\left\{\frac{(2n+1)\pi}{2a}x\right\} \cosh\left\{\frac{(2n+1)\pi}{2a}(z+h)\right\} \tag{1}$$

where

$$\omega_n^2 = g\frac{(2n+1)\pi}{2a}\tanh\left\{\frac{(2n+1)\pi}{2a}h\right\} \quad , \quad C_n = \frac{\omega K_n}{(\omega_n^2 - \omega^2)} \quad , \quad A_n = -C_n - \frac{K_n}{\omega} \tag{2}$$

$$K_n = \frac{\omega A}{\cosh\left\{\frac{(2n+1)\pi h}{2a}\right\}} \frac{2}{a}\left(\frac{2a}{(2n+1)\pi}\right)^2 (-1)^n \quad , \quad A = \epsilon_0\omega \tag{3}$$

The second order potential Φ_2 must satisfy the inhomogeneous free surface condition

$$\frac{\partial^2\Phi_2}{\partial t^2} + g\frac{\partial\Phi_2}{\partial z} = -\frac{\partial}{\partial t}\left[\left(\frac{\partial\Phi_1}{\partial x}\right)^2 + \left(\frac{\partial\Phi_1}{\partial z}\right)^2\right] + \frac{1}{g}\frac{\partial\Phi_1}{\partial t}\frac{\partial}{\partial z}\left(\frac{\partial^2\Phi_1}{\partial t^2} + g\frac{\partial\Phi_1}{\partial z}\right) \quad \text{on} \quad z = 0 \tag{4}$$

the wall condition

$$\frac{\partial\Phi_2}{\partial x} = -\epsilon_0 \sin(\omega t)\frac{\partial^2\Phi_1}{\partial x^2} \quad \text{on} \quad x = \pm a \tag{5}$$

and the bottom condition $\frac{\partial \Phi_2}{\partial z} = 0$ on $z = -h$. Further the second order part of the free surface elevation has to satisfy $\int_{-a}^{a} \zeta_2 dx = 0$. Here

$$\zeta_2 = -\frac{1}{g}\left(\frac{\partial \Phi_2}{\partial t} + \frac{1}{2}[(\frac{\partial \Phi_1}{\partial x})^2 + (\frac{\partial \Phi_1}{\partial z})^2] + \zeta_1 \frac{\partial^2 \Phi_1}{\partial z \partial t}\right)\Big|_{z=0} \tag{6}$$

A possible solution for the second order potential is

$$\begin{aligned}\Phi_2 &= \sum_{n=1}^{\infty} P(t)_n \cos(\frac{n\pi x}{a}) \cosh[\frac{n\pi(z+h)}{a}] + B(t) \\ &- \frac{\pi A}{4a\omega}(A_0 \sin[(\omega+\omega_0)t] + A_0 \sin[(\omega-\omega_0)t] + C_0 \sin(2\omega t)) \cos(\frac{\pi x}{2a}) \cosh[\frac{\pi(z+h)}{2a}]\end{aligned} \tag{7}$$

where

$$P(t)_n = P_n^1 \sin[(\omega+\omega_0)t] + P_n^2 \sin[(\omega-\omega_0)t] + P_n^3 \sin(2\omega t) + P_n^4 \sin(2\omega_0 t) \tag{8}$$

$$B(t) = B^1 \sin[(\omega+\omega_0)t] + B^2 \sin[(\omega-\omega_0)t] + B^3 \sin(2\omega t) + B^4 \sin(2\omega_0 t) \tag{9}$$

Only the dominant term of the series solution for Φ_1 is used in Eqs. 4 and 5 when finding Φ_2. By substituting

$$C^i = \begin{cases} 1 & i = 1,2,3 \\ 0 & i = 4 \end{cases} \quad D^i = \begin{cases} A_0 & i = 1,2,4 \\ C_0 & i = 3 \end{cases} \quad H^i = \begin{cases} \omega_0^2 & i = 1,2,4 \\ \omega^2 & i = 3 \end{cases} \tag{10}$$

$$F^i = \begin{cases} \omega+\omega_0 & i=1 \\ \omega-\omega_0 & i=2 \\ 2\omega & i=3 \\ 2\omega_0 & i=4 \end{cases} \quad G^i = \begin{cases} \omega\omega_0 & i=1 \\ -\omega\omega_0 & i=2 \\ \omega^2 & i=3 \\ \omega_0^2 & i=4 \end{cases} \quad E^i = \begin{cases} C_0 A_0 & i=1,2 \\ \frac{C_0^2}{2} & i=3 \\ \frac{A_0^2}{2} & i=4 \end{cases} \tag{11}$$

the expressions for the coefficients P_n^i and B^i are found as

$$\begin{aligned}P_n^i &= C^i \frac{AD^i}{a} \frac{\cosh[\frac{\pi h}{2a}]}{\cosh[\frac{n\pi h}{a}]} \frac{1}{[\frac{n\pi g}{a}\tanh[\frac{n\pi h}{a}] - (F^i)^2]} \left(\frac{(-1)^n(1+4n^2)}{(1+2n)^2(1-2n)^2} \frac{\omega(2aH^i \tanh[\frac{\pi h}{2a}] - \pi g)}{g\pi} \right. \\ &+ \left. \frac{(-1)^{n+1}}{(2n-1)(2n+1)} \left[2F^i + \frac{-(F^i)^2 + \frac{\pi g}{2a}\tanh[\frac{\pi h}{2a}]}{\omega} \right] \right) \\ &+ J^n \frac{E^i F^i \pi}{16ga^2} \frac{\cosh^2[\frac{\pi h}{2a}]}{\cosh[\frac{\pi h}{a}]} \cdot \frac{(3\pi g - 2aG^i \tanh(\frac{\pi h}{2a}) - 2\pi g \tanh^2(\frac{\pi h}{2a}))}{-(F^i)^2 + \frac{g\pi}{a}\tanh[\frac{\pi h}{a}]} \quad i = 1 \cdots 4\end{aligned} \tag{12}$$

where $J^n = 1$ for $n = 1$ and $J^n = 0$ for $n > 1$. Further

$$\begin{aligned}B^i &= -\frac{AD^i \omega}{2g\pi a} \frac{\cosh[\frac{\pi h}{2a}]}{(F^i)^2}(2aH^i \tanh[\frac{\pi h}{2a}] - \pi g) - \frac{AD^i}{a(F^i)} \cosh[\frac{\pi h}{2a}] \\ &+ \frac{AD^i}{2a\omega} \cosh[\frac{\pi h}{2a}](1 - \frac{g\pi}{2a(F^i)^2} \tanh[\frac{\pi h}{2a}]) \\ &- \frac{E^i}{16ga^2(F^i)} \pi \cosh^2[\frac{\pi h}{2a}](\pi g + 2aG^i \tanh(\frac{\pi h}{2a}) + 2\pi g \tanh^2(\frac{\pi h}{2a})) \quad i = 1,2,3\end{aligned} \tag{13}$$

$$B^4 = -\frac{E^i}{16ga^2(F^i)} \pi \cosh^2[\frac{\pi h}{2a}](\pi g + 2aG^i \tanh(\frac{\pi h}{2a}) + 2\pi g \tanh^2(\frac{\pi h}{2a})) \tag{14}$$

The B^3 coefficient contains an additional term $-A^2/(4\omega^2)$. The solution has been verified by checking that Φ_2 satisfies the boundary conditions. The presented solution satisfies $\Phi_2 = 0$ for $t = 0$ while ζ_2 is initially non-zero. A more general solution for Φ_2 can be obtained by adding solutions that satisfy the homogeneous free surface condition and body boundary conditions.

Fig. 2 shows a cross-section of the tank used in the experiments. The tank was forced to oscillate in the horizontal direction in the cross-sectional plane. The length of the tank was 0.20 m, and as long as no plunging wave breaking occurred, the flow was close to two-dimensional even for long time simulations. The excitation was sinusoidal in time after an initial phase. This initial phase lasted for approximately two oscillation periods.

The low damping in the tank made it inconvenient to wait for the motion from the last simulation to die out totally before a new run was started. Measurements of the free surface at the positions shown in Fig. 2 were made, and pictures were taken at registered time instants. The sampled time series are 50 seconds long, but video recordings of longer simulations, as long as 5 minutes, showed that the pronounced beating was still present and steady state oscillations with the forced oscillation period was not achieved. This shows that the damping of the fluid motion is even lower than Keulegan found. One reason may be scale effects. Keulegan assumed laminar flow and used smaller models than us. The Reynolds number associated with the boundary layer flow in our experiments suggests turbulent flow.

As a general comment to the experiments, we note the obvious nonlinearity present in the free surface elevation; the increase in crest height and decrease in wave trough relative to a sinusoidal standing wave. Figs. 3 and 4 show the measured and calculated free surface elevation at wave probe FS3 (see Fig. 2) for $h = 0.5$m, forced oscillation period $T = 1.4$s and $\epsilon_0 = 0.047$m. Fig. 5 shows the position of the tank during the first 20 seconds of this simulation. $t = 0$ corresponds to the same time instant in Figs. 3 and 5. The excitation of the tank started at $t = 7.5$s. The first natural period for this situation is $T_0 = 1.75$s. Fig. 3 shows that the free surface is initially in motion. This gives different initial conditions for the simulation (Fig. 4) and the experiment. Also the excitation with an initial phase of an increasing amplitude will lead to differences in the response. The comparison between the measured and calculated free surface elevation at FS3 shown in Fig. 6 is done for a time window after a few initial oscillations. The calculated values are shifted in time so that the zero-crossings of the fast oscillating part and slowly varying envelope match. The 2. order solution gives a better agreement for both the wave trough and wave crest than the 1. order solution. The influence of initial conditions and non-harmonic excitation will be investigated systematically. We should note that the oscillation amplitude of the free surface is clearly larger than the excitation amplitude.

The free surface profile found from the experiments is compared in Fig. 7 with the 1. order and 2. order approximations and with calculations based on the combined numerical and analytical steady-state solution of Solaas and Faltinsen [2]. Here $h = 0.5$m, $T = 2.0$s and $\epsilon_0 = 0.051$m. The time instant is just before the maximum free surface elevation is reached at the right side wall. We see a tendency to wave breaking at the wave crest. Only the dominant term in the series solution of Φ_1 is included in Eq. 6 when calculating ζ_2. This is consistent with keeping only this term when deriving Φ_2.

The second order solution agrees best with the experiments, but there are differences left to explain. We note spilling wave breaking in the experiments. According to Penney and Price [4], a criterion for wave breaking of a standing wave is a vertical downward acceleration larger than 1 g. In the simulation corresponding to Fig. 8, we get a maximum downward acceleration of 1.6 g. Higher order harmonics left out in the theory are more important for acceleration than for displacement.

When the forced oscillation period is close to the highest natural period of the fluid motion inside the tank, the water hits the tank ceiling even for very small excitation amplitudes. A more direct numerical method may then be needed. Since local damage due to water impact on the tank ceiling is of concern and hydroelasticity matters in this context, the chosen numerical method must include the effect of dynamic elastic vibrations of the structure. Since long numerical simulations are needed to get proper statistical estimates of the tank behavior in a seaway, it may be worthwhile to use an analytically based method when the water does not hit the tank ceiling. It implies that the presented analytical solution should be generalized to satisfy arbitrary initial conditions.

Acknowledgements

This work is part of a Ph. D. thesis sponsored by the Research Council of Norway and Det Norske Veritas.

References

[1] Faltinsen, O. M., 'A Nonlinear Theory of Sloshing in Rectangular Tanks', *Journal of Ship Research*, Vol. 18, No. 4, Dec. 1974, pp. 224-241

[2] Solaas, F. and Faltinsen, O. M., 'Combined Numerical and Analytical Solution for Sloshing in Two-dimensional Tanks of General Shape', *Journal of Ship Research*, Vol. 41, No. 2, June 1997

[3] Keulegan, G. H., 'Energy Dissipation in Standing Waves in Rectangular Basins', *Journal of Fluid Mechanics*, Vol. 6, 1958

[4] Penney, W. G. and Price, A. T., 'Finite Periodic Stationary Gravity Waves in a Perfect Liquid', *Philosophical Transactions of the Royal Society* (London), Vol. A 244, 1952, pp. 254-284

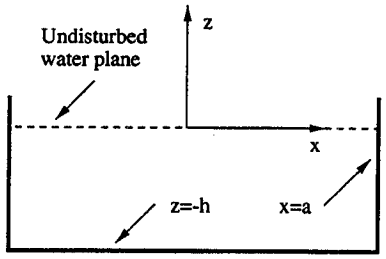

Figure 1: Coordinate system

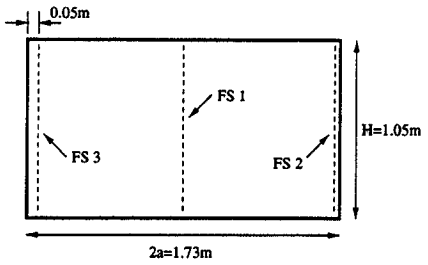

Figure 2: Tank used in the experiments.

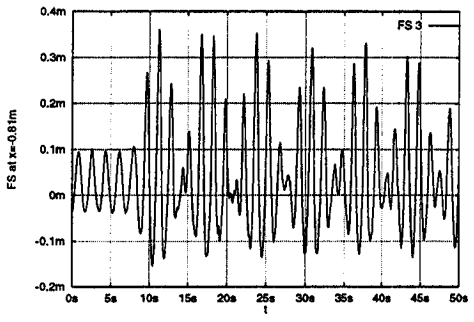

Figure 3: The measured free surface elevation at wave probe FS3 for $h = 0.5$m, $T = 1.4$s and $\epsilon_0 = 0.047$m.

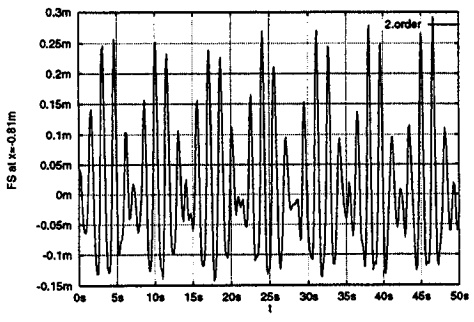

Figure 4: The calculated free surface elevation at the position of wave probe FS3 for $h = 0.5$m, $T = 1.4$s and $\epsilon_0 = 0.047$m.

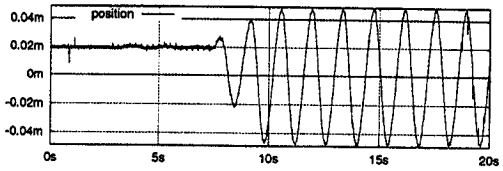

Figure 5: The position of the tank during the measurement presented in Fig. 3.

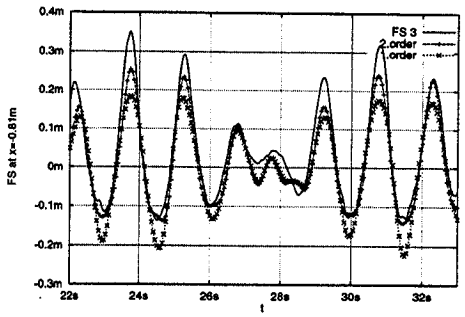

Figure 6: A comparison between the measured and calculated free surface. The conditions are as in Fig. 3.

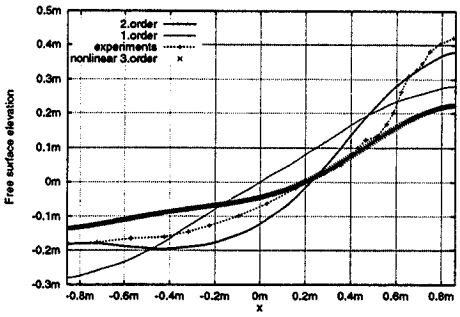

Figure 7: The free surface profile found from the experiments compared with the 1. and 2. order approximations and with calculations based on the combined numerical and analytical solution of Solaas and Faltinsen [2] $h = 0.5$m, $T = 2.0$s and $\epsilon_0 = 0.051$m.

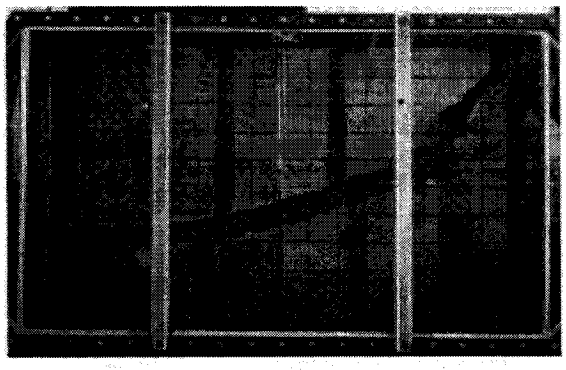

Figure 8: Picture of the sloshing tank for $h = 0.5$m and $T = 2.0$s.